Int. J. Electrochem. Sci., 13 **(2018)** 4100 – 4114, doi: 10.20964/2018.05.73

International Journal of ELECTROCHEMICAL SCIENCE
www.electrochemsci.org

Differential Pulse Stripping Voltammetric Determination of Metronidazole with Graphene-Sodium Dodecyl Sulfate Modified Carbon Paste Electrode

Mingfang Zhu[1,*], *Hongqing Ye*[1], *Mushen Lai*[1], *Jianshan Ye*[2], *Jiemin Kuang*[1], *Yuping Chen*[1], *Jingyue Wang*[1], *Qianyi Mei*[1]

[1] College of Pharmacy, Guangdong Pharmaceutical University, Guangzhou higher education mega center, Guangzhou 510006,
[2] School of Chemistry and Chemical Engineering, South China University of Technology, Wushan, Guangzhou 510640,
[*]E-mail: zhumfgy@126.com

Received: 6 January 2018 / *Accepted:* 11 March 2018 / *Published:* 10 April 2018

A sensitive electrochemical sensor using graphene self-assembled sodium dodecyl sulfate (SDS) as a composite membrane modified carbon paste electrode was developed for the detection of metronidazole (MNZ) using voltammetry. And the electrochemical properties of the composite membranes were studied by electrochemical impedance spectroscopy and chronocoulometry. At the optimum conditions, the concentration of MNZ was determined using oxidation peak by differential pulse stripping voltammetry (DPSV) in the linear range of 0.08 to 200 μM with a detection limit of 8.5 nM. The high sensitivity, wider linear range, good reproducibility and the minimal surface fouling made the modified electrode suitable for determining MNZ concentrations in biological samples and tablets. Good recovery results were obtained.

Keywords: Metronidazole; Graphene; Sodium dodecyl sulfate; Modified carbon paste electrode; Voltammetry

1. INTRODUCTION

Metronidazole (MNZ), as an antibiotics, has been widely used for cure or prevention of diseases coming from anaerobic bacteria or protozoa infection in human beings [1,2]. It is also used as the growth promoters in agriculture, aquaculture, livestock and bee-keeping for its low-price and effective veterinary drug. Because of their potential toxicity in human health, many countries like the

European Union (EU), American and China have prohibited their uses in food and animal feeds. In addition, large-scale abused of antibiotics have caused water environmental problems and food safety issues. Hence, it is very important to detect metronidazole sensitively and accurately in biological and environmental samples.

So far, the methods for determination of MNZ in various samples mainly include high performance liquid chromatography [3,4], liquid chromatography-mass spectrometry [5-7], spectrophotometry [8-11], fluorescent nanosensor [12], nuclear magnetic resonance spectroscopy [13], electrophoresis [14] and electrochemical analysis methods [15-18]. In all these methods, electrochemical techniques have been widely used to determinate MNZ for its low cost, high sensitivity and rapid response. Some electrodes with different modifying materials are prepared for the MNZ determination such as molecularly imprinted polymer [15,19], copper-poly(cysteine) film [20], 3D gold nanotube [21], carbon nanotube [18,22] and graphene [23,24]. Because graphene has unique electronic structure and large surface area, graphene-based electrode exhibits superior electrocatalysis properties [25].

Sodium dodecyl sulfate (SDS), a kind of anionic surfactant, which provides negative charges, can not only avoid aggregation of CNTs and GR but also improve the water solubility of the nanomaterials [26-28]. In addition, SDS can interact with some molecules through electrostatic function to promote the electron transfer between the electrodes and the molecules in the solution. Thus, the sensitivity and selectivity of the analysis are improved [28-30].

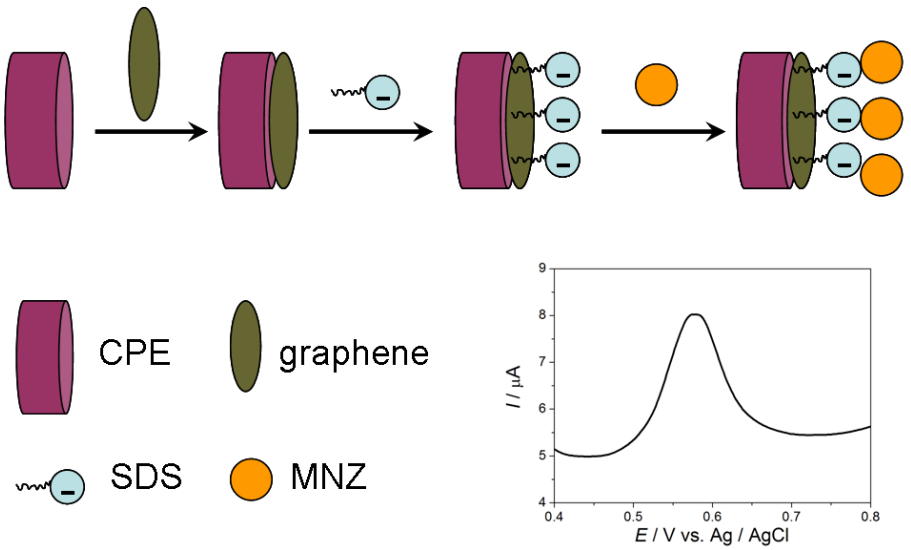

Scheme 1. Schematic illustrations of the preparation processes of the electrode for the determination of MNZ.

As is well known, MNZ contains a nitro group, which is an electrochemically active reducible center, so four electron irreversible reduction of the nitro group of MNZ had been widely reported [15,31-35] . However, according to Mollamahale's report [21], when scanning the potential from -0.15 V to -1.0 V, and then in the reverse sweep, also by following the scan from 0.5 V toward negative direction, a pair of redox peaks were appeared at 0.25 V and 0.15 V, respectively. So their group used

the oxidation peak of the MNZ reduction product for analytical determination. Meanwhile, Brett's research [36] shown that when the cyclic voltammetric scan was initiated in the positive potenial from -0.2 V to 0.8 V, and then in the reverse scan from 0.8 V to -1.0 V and again to 0 V, three oxidative peaks and two reduced peaks are observed. In this paper, we provided a convenient method to construct the SDS functionalized GR carbon paste electrode based on the oxidation peak of MNZ, the fabrication process for a new MNZ electrochemical sensor as shown in scheme 1. Firstly, graphene was dropped on the carbon paste electrode, and then SDS self-assembled on the surface of graphene by van der Waals forces. The constructed sensors by self-assembly method yielded sensitive and selective determination of MNZ, the effects of main experimental variables such as pH, stripping potential and time were systematically discussed. The sensors remain contented repeatability and stability. Finally, the sensors were applied for accurate determination of MNZ concentration in tablets and animals samples.

2. EXPERIMENTAL

2.1 Reagents and solutions

MNZ was purchased from Chinese Drug and Biological Products (Guangzhou, China). SDS, cetyltrimethylammonium bromide (CTAB) and Triton X-100 were provided by Bio Life Science & Technology Co. Ltd (Shanghai, China). Potassium hexacyanoferrate (Ⅱ) ($K_4[Fe(CN)_6]$) and potassium hexacyanoferrate (Ⅲ) ($K_3[Fe(CN)_6]$) were bought from Guangzhou chemical reagents factory. Graphite powder, liquid paraffin oil and silicon oil were purchased from Sinopharm Chemical Reagent Co. Ltd. (Shanghai, China). Graphene was synthesized by the chemical oxidation-reduction treatment of graphite according to our previous work [37]. Other chemicals were of analytical reagent grade and used without further purification.

1mM MNZ ethanol-water stock solutions were prepared before use. All MNZ working solutions were prepared by dilution of these stock solutions with acetic acid - sodium acetate buffer solution (0.1M, pH 4). 1mg mL^{-1} graphene solution was dispersed 1mg graphene into 1ml N,N-dimethylformamide (DMF) to obtain a homogeneous black dispersion by sonicate for 1 h. SDS and other solutions were prepared by dissolving the necessary quantity of reagent in water. Aqueous solutions were prepared with ultrapure water.

2.2 Apparatus and measurement

A scanning electron microscope (NoVaTM Nano SEM 430, FEI Company, Netherlands) was used for observation of the graphene and SDS functionalized graphene. Electrochemical impedance spectroscopy, cyclic voltammetry (CV), differential pluse stripping voltammetry (DPSV) and chronocoulometry experiments were conducted on an Ingsens 4030 Electrochemical Workstation (Guangzhou Ingsens Sensor Technology Co. Ltd., China) with a three-electrode-system which consists of homemade modified carbon paste working electrode (i. d. 3 mm), platinum counter electrode and

Ag/AgCl reference electrode. The pH values were determined by pH meter (pHS-3C, Shanghai REX Instrument Factory, China). All experiments were performed at room temperature (ca. at 25°C).

The frequency of 0.1Hz to 0.1MHz was used for electrochemical impedance spectroscopy determination in the solution of 5 mM $K_3Fe(CN)_6$ / $K_4Fe(CN)_6$ containing 0.1 mM KCl. Cyclic voltammetry was carried out with 50 μM metronidazole from 0 ~1.0 V at the scan rate of 100 mVs^{-1} in HAc-NaAc buffer solution (pH 2.5). Quantification determination for different MNZ concentrations was applied by DPSV with accumulation potential of -0.2 V and the accumulation time of 30 s, increasing potential, pulse amplitude, pulse width, sample width and pulse period were chosen of 9 mV, 50 mV, 25 ms, 20 ms, 50 ms, respectively. Chronocoulometric curve was recorded in the solution of 2.5 mM $K_3 Fe (CN)_6$ containing 0.1 mM KCl with pulse width of 10 s and sample interval of 0.1 s.

2.3 Electrode preparation

After determinating the optimum ratio of graphite powder to binder, the carbon paste electrode (CPE) was prepared by mixing the graphite powder, liquid paraffin oil and silicon oil in the ratio of 65:25:10 (w/w/w). A mortar and pestle were used to obtain a homogeneous paste. The prepared paste was tightly packed into the cave of the plastic tube (i.d. 3 mm). A copper rod inserted into the paste provided the electrical contact. The paste then was polished on a weighing paper to get smooth surface. Similarly, graphene modified CPE (GR/CPE) was prepared by dropping 5 μl GR onto the surface of CPE using pipette, and then it was allowed to dry at room temperature. The GR/CPE was immersed into the 0.1% (w/w) SDS for two minutes to obtain the SDS-graphene modified carbon paste electrode, which was designated as SDS-GR/CPE. To renew the surface of electrode, pushing an excess of the paste out of the tube and polishing it on the weighing paper, then a new CPE was obtained. For GR/CPE and SDS-GR/CPE, it may be modified again at the renewed CPE.

2.4 Preparation of samples

MNZ tablets were purchased from local drugstore in Guangzhou city. 10 Tablets were taken randomly, powdered and then weighted a quantity of the powder equivalent to one tablet, dissolved with ultrapure water and accurately transferred to a 100 mL volumetric flask, diluted to scale. And the resulting solution was diluted with ultrapure water to obtain the working sample solution.

Healthy Shrimps were obtained at local market in Guangzhou city and were cultured in the water containing a certain amount of MNZ for two hours. After that, 3g shrimp meat of the removed shrimp shell was homogenized with 10 ml methanol. Methanol was then added into the homogenate at a volumetric ratio of 1:1 to eliminate protein [18]. This step was followed by centrifugation. The supernatants were evaporated to dryness using nitrogen. And then it was dissolved with acetic acid - sodium acetate buffer solution (0.1M, pH 4) for use in this experiment. For the spiked recovery experiment, a certain quantity of MNZ was added into the samples through the homogenization.

3. RESULTS AND DISCUSSION

3.1 Surface Characterization of SDS-GR and Electrochemical characterization of electrodes

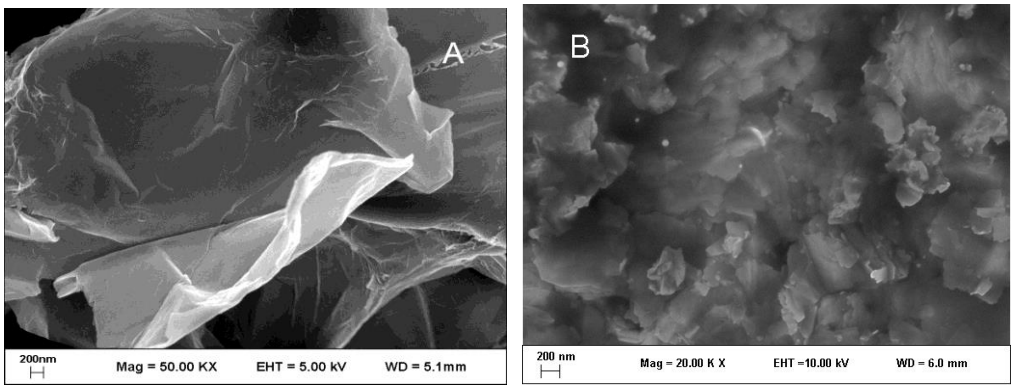

Figure 1. SEM images of GR (A) and SDS-GR (B)

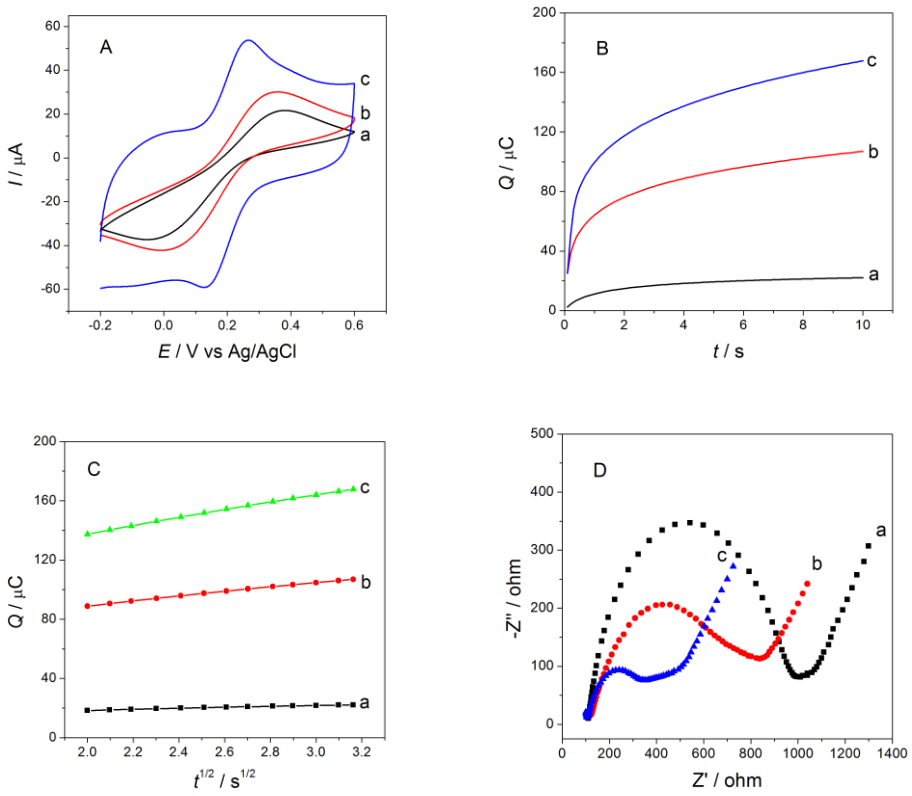

Figure 2. (A) CVs, (B) Chronocoulometric curves and (C) the linear regressions of Q vs. $t^{1/2}$ recorded in the solution of 2.5 mM $K_3Fe(CN)_6$ containing 0.1 mM KCl at CPE (a), GR/CPE (b) and SDS-GR/CPE (c). (D) Nyquist plots in the solution of 5 mM $K_3Fe(CN)_6$ / $K_4Fe(CN)_6$ containing 0.1 mM KCl at CPE (a), GR/CPE (b) and SDS-GR/CPE (c).

The surface characterizations of GR and SDS-GR from SEM analysis were illustrated in Fig. 1. Obviously, the surface morphology of the SDS-GR is much different from those of GR. As shown in Fig. 1A, the GR with the shapes of flowers-like and crimples were observed, which could

provide high surface area and benefit the surfactant to be adsorbed on the surface of GR. Whereas, some small nanospheres attached on the surface of GR flake in Fig.1B, indicating that SDS-GR were assembled successfully and it may supply larger surface area to enhance the electrocatalytic capacity. The structure of SDS-GR is beneficial to detect analytes sensitively.

Cycle voltammetry characterizations of CPE, GR/CPE and SDS-GR/CPE were investigated with the redox probe $K_3[Fe(CN)_6]$ at the scan rate of 100 mVs^{-1} as shown in Fig.2A.

It can be clearly seen that, the current response for the $K_3[Fe(CN)_6]$ at SDS-GR/CPE (Fig.2A, curve c) was largely increased, and the current intensity arranged in order from large to small was SDS-GR/CPE (Fig.2A, curve c) > GR/CPE (Fig.2A, curve b) > CPE (Fig.2A, curve a), indicating that the electrochemical active sites of CPE increased by GR surface modification [38,39] . And the largest current at the SDS-GR/CPE could be ascribed to the electro-catalytic capacity of GR and large surface areas of SDS-GR. Moreover, the difference between E_{pa} and E_{pc} (ΔE_p) at the GR/CPE and SDS-GR/CPE is smaller than that at the CPE, suggesting that GR facilitate the fast electron transfer, which was due to the reactive edge plane defects on graphene [40]. In addition to the above reasons, chemical affinity interaction between SDS with $K_3[Fe(CN)_6]$ might be another factor for the quasireversible redox process at the SDS-GR/CPE [41].

The effective electrochemical electrode areas of CPE, GR / CPE, SDS-GR / CPE were estimated by the chronocoulometry. The chronocoulometric curves (Fig.2B) were measured in 2.5 mmol L^{-1} $K_3[Fe(CN)_6]$ solution containing 0.1 mol L^{-1} KCl, and the relationships between Q and $t^{1/2}$ (Fig.2C) were expressed as:

Q (CPE) = 3.26 $t^{1/2}$ + 12.01 (r = 0.9952)，Q (GR / CPE) = 15.52 $t^{1/2}$ + 18.86 (r =0.9988), Q (SDS-GR / CPE) = 26.05 $t^{1/2}$ + 86.01 (r = 0.9992);

According to the Anson equation [42],

$$Q = \frac{2nFAcD^{1/2}t^{1/2}}{\pi^{1/2}} + Q_{dl} + Q_{ads}$$

In the formula, n is the number of electron transfer (for $K_3[Fe(CN)_6]$, n = 1), F refers to the Faraday constant, A represents the active area of working electrode, c is the concentration of analyte, D means the diffusion coefficient of $K_3[Fe(CN)_6]$ (7.6×10^{-6} cm^2/s) , Q_{dl} is double-layer charge and Q_{ads} is the Faraday charge. Because of the different value of the slope derived from the regression equation of Q - $t^{1/2}$, the electrode active areas of the CPE, GR/CPE and SDS-GR/CPE were calculated to be 4.34 mm^2, 20.69 mm^2, 34.73 mm^2, respectively. Among them, the SDS-GR/CPE displayed 8 times the electrode areas than that of the unmodified CPE, which indicated that the enlarged active areas of the modified composite resulted in the outstanding electrochemical characteristics.

In order to further study the surface electron transfer of electrodes, we use electrochemical impedance spectroscopy (EIS) to investigate the impedance change of the different modified electrodes surface. The EIS graph usually shows a semicircular curve at higher frequencies and a linear curve at lower frequencies, which represent the electron transfer resistance and diffusion process, respectively [43]. Fig.2D displayed the Nyquist diagram of CPE (Fig.2D, curve a), GR/CPE (Fig.2D, curve b) and SDS-GR/CPE (Fig.2D, curve c) in the solution containing of 0.1 M KCl and 5 mM $K_3[Fe(CN)_6]$ / $K_4[Fe(CN)_6]$. It was obvious that both GR/CPE and SDS-GR/CPE have smaller R_{ct} in comparison to the CPE. That is to say, GR and SDS-GR membranes have higher electrochemical

activity to make the electron transfer faster. These results also indicate that GR and SDS-GR are well adhered to the surface of the CPE.

3.2 Cyclic voltammetric studies of MNZ

According to Brett's research, when preconcentration potential is lower than the reduction potential of MNZ, the substance of preconcentration on the electrode is not the original compounds but the reduction products [36]. So when preconcentration at the potential of -0.4V, the electrochemical behaviors of MNZ at different electrodes were then studied in pH 4 HAc-NaAc buffer solution by CV and the cyclic voltammograms were shown in Fig.3.

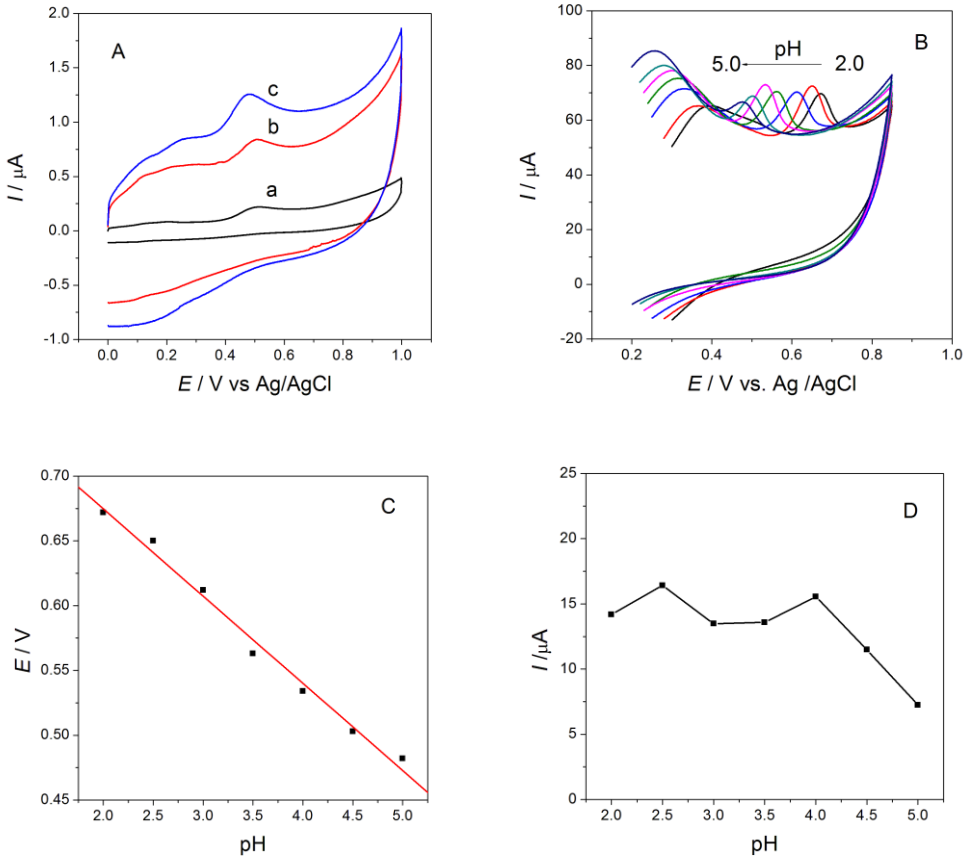

Figure 3. (A) CVs of 50 μM metronidazole in HAc-NaAc buffer solution (pH 2.5) at CPE (a), GR/CPE (b) and SDS-GR/CPE (c). （B）CVs of 200 μ M metronidazole at the SDS-GR/CPE in HAc-NaAc buffer solution with different pH values of 2.0, 2.5, 3.0, 3.5, 4.0, 4.5, 5.0 (from right to left). (C) Peak potential with respect to pH. (D) Peak current with respect to pH. Scan rate: 100 mVs^{-1}.

It can be seen that at the scan potential range of 0 ~1.0 V, and then in the reverse direction, a poor response can be seen at the CPE (Fig.3A, curve a), showing its insensitivity toward MNZ. An improved voltammetric response with peak potential and peak current appeared at the GR/CPE (Fig.3A, curve b), indicates the suitability of GR with large surface area and good electronic

conductivity as an electrode decorated material. However, an reversible redox peaks and an oxidation peak were observed at the SDS-GR/CPE (Fig.3A, curve c), this is in line with the literature [21,36]. The redox peaks at 0.26 V and 0.17 V corresponded to the reversible redox behavior of the hydroxylamine group of the reduced form of MTZ, and the oxidation peak at 0.477 V attributed to the oxidation behavior of the hydroxylamine and the nitroso derivative. The possible electrochemical redox mechanism of MTZ can be shown in the following reaction.

$$R\text{-}NO_2 + 4e^- + 4H^+ \rightarrow RNHOH + H_2O \quad (1)$$

$$RNHOH \overset{+2e \quad +2H^+}{=\!=\!=\!=\!=\!=} RNO \quad (2)$$

$$RNHOH + RNO \rightarrow RNO{=}NR + H_2O + 2e^- + 2H^+ \quad (3)$$

Due to the preferable potential and high current response, the oxidation peak at 0.477V had been used for further investigation.

3.3 Effect of pH value and scan rate

In order to study the effect of pH value on the peak potentials and the peak currents of the electrochemical oxidation of MNZ at the SDS-GR/CPE, the peak signals were recorded at the HAc-NaAc in the pH range from 2.0 to 5.0 using cycle voltammetry at the scan rate of 100 mV s^{-1}. As shown in Fig.3B, the oxidation peak potentials shifted in the negative direction with an increase in pH, illustrating that hydrogen ions are participated in this electrochemical oxidation reaction. The relationship between anodic peak potential and pH is shown in Fig.3C, and the regression equation was expressed as E = -0.0673pH + 0.809 (E is in V, R = 0.9944) with a slope of 67.3 mV per pH unit, the slope was closed to the theoretical value of 59 mV/pH at 25ºC expected from the Nernst equation, which demonstrated that the electrochemical process of MNZ was proton dependent in the pH range from 2.0 to 5.0 and electron transfer is associated with equal proton transfer. As can be seen from Fig.3D, peak currents increased at pH 2.5, then decreased and reached to a platform at pH 3.0-3.5, subsequently, increased again at pH 4.0 and decreased when the pH values exceeded 4.0. Considering both the electrode stability and the detection sensitivity, the pH value of buffer solution was chosen pH 4.0 for the following measurements.

To further investigate the kinetics of electrode reaction, the effects of scan rate on the oxidation peak current and peak potential were studied with cyclic voltammetry.

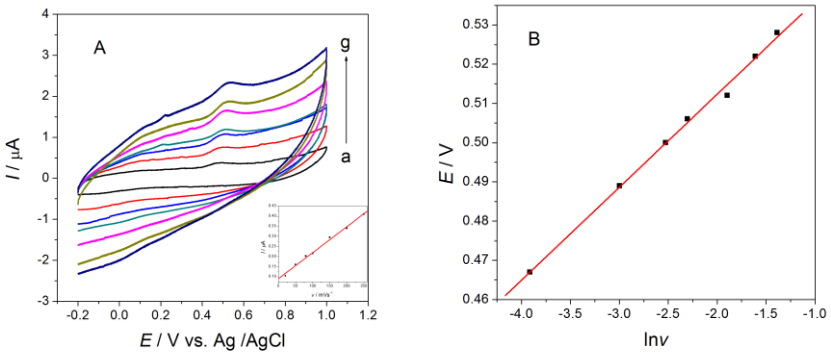

Figure 4. (A) CV of 50 μM metronidazole at the SDS-GR/CPE in HAc-NaAc buffer solution (pH 2.5) at different scan rate. (a – g): 20, 50, 80,100,150, 200 and 250mVs^{-1}. The insert shows the linear relationship between scan rate and the oxidation peak current. (B) The plots of the peak potential vs. the logarithm of the scan rate.

As shown in Fig. 4A, the scan rate of cyclic voltammetry exhibits an obvious effect on the oxidation peak currents of MNZ, and the anodic peak currents increased linearly as the scan rate increased in the range of 20-250 mVs^{-1} (Fig.4A insert diagram) with the regression equation of I_p (μA)= 0.00128 v (mVs^{-1}) + 0.0909 (R = 0.9965).It is suggested that the electrode reaction of MNZ at the SDS-GR/CPE was adsorption-controlled processes.

Furthermore, the electrochemical oxidation peak potential shifted positively while increasing the scan rates. A linear relationship between E_p and the logarithm of the scan rate can be expressed as follows: E_p (V) = 0.0237 ln v (Vs^{-1}) + 0.5597 (r =0.9981). For an irreversible electrode process, Ep can be defined by the following equation at 25 °C according to Laviron's theory [44] :

$$E_p = E^0 + \frac{RT}{\alpha nF}\ln\frac{RTk^0}{\alpha nF} + \frac{RT}{\alpha nF}\ln v \ .$$

Where E_p is the peak potential, E^0 stands for the standard potential, R means the gas constant (8.314 J K^{-1} mol^{-1}), T refers to the absolute temperature (K), F represents the Faraday constant (96485 C mol^{-1}), α is the charge transfer coefficient, n is the electron transfer number of rate-determining step, k^0 is standard rate constant of the reaction, and v is scan rate. From the slope (0.0237) of E_p versus ln v, αn value is 1.08. In general, α is granted to be 0.5, the number of electron transfer was found to be 2, and the number of proton in the electrode reaction was also 2. Whereas E^0 was 0.446 by extrapolating curve of E_p versus v to the vertical axis at v = 0. From $E°$ =0.446, the slope = 0.0237 and the intercept value of E_p vs. ln v = 0.5597, k^0 is calculated to be 3.27 ×10^3 s^{-1}.

3.4 Effect of the SDS on the electrooxidation of MNZ

It is well known that surfactants play the important role in reducing the aggregation of GR, the electrode surface modification and antifouling ability. Thus, different surfactants such as SDS, cetyltrimethylammonium bromide (CTAB) and Triton X-100 were performed to detect the peak current intensity for MNZ oxidation. Among these surfactants, CTAB and Triton X-100 displayed the

decreased peak currents intensity, while SDS exhibited the better electrochemical changes both in the enhancing the peak currents intensity and in the reducing the overpotential to make the peak potential shift to the less positive direction. The main reason for this lies in the head groups and the alkyl chains length of the surfactants [45, 46]. Hence, surfactants accumulate the substrates with opposite charges and repulse the species with the same charges. In the pH range of our discussing, MNZ exists mainly in the cationic form [47], but CTAB is a cationic surfactant and Triton X-100 is a neutral surfactant, so CTAB may repulse MNZ and Triton X-100 may hinder the formation of adsorb layer.

SDS as an anionic surfactant can adsorb on the positively charged electrode surface [48] and helps the accumulation of molecules especially when it is in cationic form [49]. At pH < 7, the hydroxylamine groups of the reduced form of MTZ are protonated [16], so the protonated hydroxylamine could easily adsorb on the SDS to form an ion pair to reduce the distance from MNZ to electrode surface, thus yielded higher currents. It is found that when the time for SDS adsorption on the GR surface for 2 minutes, the oxidation peak current reached maximum value, and then it decreased with the increase of the adsorption time. The results may be because of the aggregate formation of SDS at concentrations below the critical micelle concentration of the pure surfactant in the presence of the positively-charged drug as a cationic species [50]. So 2 minutes were chosen as the SDS adsorption time in our experiment.

3.5 Accumulation potential and accumulation time

Owing to the oxidation of MNZ was a representative adsorption-controlled process at the SDS-GR/CPE, the accumulation step could increase the amount of MNZ on the electrode surface, and then make the peak currents increased. The accumulation potential (E_{acc}) and accumulation time (t_{acc}) with different pulse stripping voltammetry (DPSV) were shown in Fig.5.

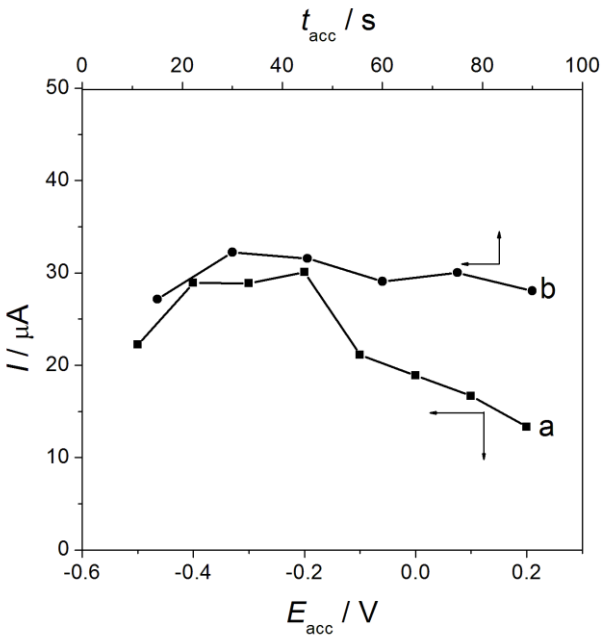

Figure 5 Effect of accumulation potential (a) and accumulation time (b) on peak currents of MNZ (50 μM) with DPSV.

It can be seen from Fig.5 curve *a* that, in the accumulation potential range from -0.5 V to 0.2 V, the peak currents increased and kept almost unchanged between -0.4V to -0.2V, and then decreased at -0.2 V to 0.2 V, so -0.2 V was chosen as accumulation potential for the further voltammetric studies of MNZ with DPSV. Accumulation time was tested over the range of 15-90 s (Fig.5, curve b), and the current increased rapidly when at the accumulation time of 30 s, then the oxidation peak current reached almost a platform from 30 s to 75 s, it is suggested that the adsorption quantity of MNZ on the SDS-GR/CPE reached saturation. In consideration of both sensitivity of the assay and working efficiency, 30 s was selected as the optimum accumulation time.

3.6 Calibration curve for determination of MNZ

Figure 6 illustrates the DPSV response of different concentrations of MNZ under optimized experimental conditions.

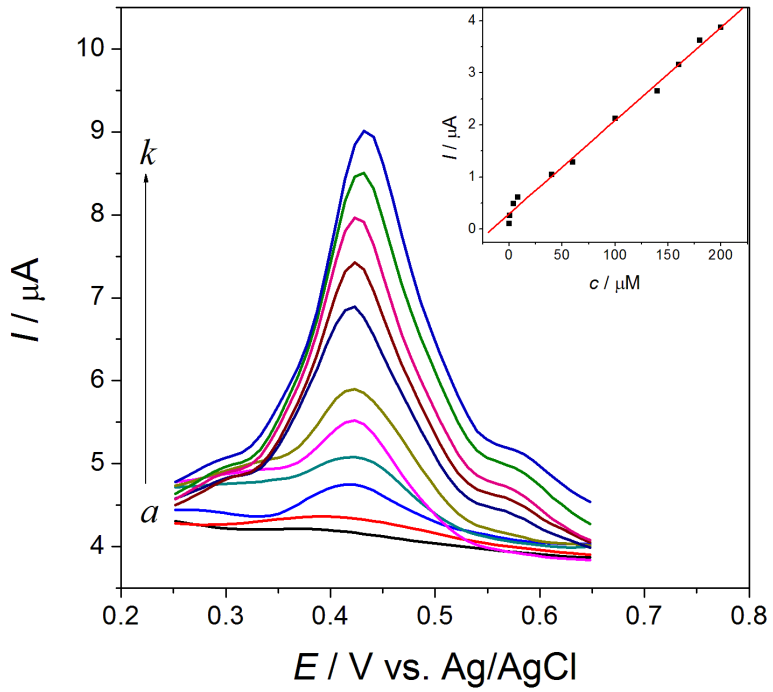

Figure 6. DPSV of SDS-GR/CPE in HAc-NaAc solution with different MNZ concentrations. For (*a* - *k*): 0.080, 0.40, 4.0, 8.0, 40, 60, 100, 140, 160, 180, 200 μM.

According to Fig.6, the corresponding regression equation was expressed as I_{pa} (μ A) = 0.0179 *c* (μ mol L^{-1}) + 0.3008 (*R* = 0.9966) in the MNZ concentrations range from 0.08-200 μ mol L^{-1} and the detection limit was estimated to be 8.5 n mol L^{-1} (3S/N). The results were in comparison with those reported in related literature and are listed in Table 1.

The method used in this paper exhibited a relatively wide linear range and low detection limit. The method was sensitive to MNZ determination and can be applied to real samples.

Table 1. Comparison of different modified electrodes for the determination of MNZ.

Electrode	Linear range(μM)	Detection Limit(μM)	Techniques	References
UTGE	3~ 90	0.142	DPV	[51]
Gr-IL/GCE	0.1 ~25	0.047	DPV	[2]
MWNT–DHP/GCE	0.025~10	0.006	DPV	[52]
β-CD-GNPs/poly(l-cys)/GCE	0.1~ 600	0.014	LSSV	[53]
Cysteic Acid/PDDA-GN/GCE	0.01~1 and 70~800	0.0023	LSV	[54]
SWCNT/GCE	0.1~200	0.063	Amperometry	[22]
BDD electrode	0.2~4.2	0.065	SWV	[16]
DMIP/CPE	0.4~200	0.091	DPV	[15]
r-GO/MCGCE	0.032~3.4	0.0012	DPV	[55]
SDS-GR/CPE	0.08~200	0.0085	DPSV	This work

3.7 Interference, repeatability and stability studies

The influence of some potential interference substances on the measurement of MNZ was studied under mentioned above optimal conditions. Some foreign species with 500 times of chloramphenicol, norfloxacin, oxytetracycline, Mg^{2+}, Co^{2+}, Zn^{2+}, Ba^{2+}, Ca^{2+}, Na^{+}, Al^{3+}, Cl^{-}, SO_4^{2-}, PO_4^{3-} and 100 fold of ascorbic acid, uric acid did not interfere with the measurement of metronidazole.

The repeatability of the SDS-GR/GCE was evaluated by measuring 5 μM metronidazole solution with the same electrode for 10 successive times and the relative standard deviation (RSD) was 4.6%, which revealed that the electrode possessed a satisfying repeatability. When the SDS-GR/GCE stored at room temperature for 10 days, only a little decrease of the current value was observed with signal change of 4.4% for MNZ, which demonstrated the good storage stability of the sensor.

3.8 Analytical applications

To further verify practical applications of the obtained electrode, the SDS-GR/CPE was used to detect MNZ in tablets and shrimp samples. The results were listed in Table 2.

Table 2. Detection of MNZ in pharmaceutical tablets and shrimps samples (n=3)

Samples	Added (μM)	Found (μM)	Recovery (%)	RSD (%)
Tablets	2	1.976	98.8	4.1
	5	4.860	97.2	2.2
	50	51.56	103.1	3.0
Shrimps	2	2.195	109.8	3.3
	5	4.561	91.2	4.5
	50	46.30	92.6	4.8

The obtained recoveries of 91.2% ~ 109.8% and standard deviations of 2.2 ~ 4.8% were satisfactory and acceptable. Thus the proposed method with SDS-GR/CPE had great potential in real sample determination and it can avoid interference from important common oxidizable substances discovered in biological samples and pharmaceutical samples.

4. CONCLUSIONS

In this paper, the SDS-GR/CPE was prepared and it was used to detect the MNZ with the azoxycompoud of the intermediates oxidation. Compared with the GR/CPE and CPE, the SDS-GR/CPE exhibits the enhanced peak current and reduces the overpotential toward the MNZ oxidation. Then, the prepared electrode has many advantages, such as simple, easy preparation and inexpensive. For electrochemical measurements of MNZ it has high stability, selectivity, reproducibility and wide linear range. In addition, the electrode can also be used to determine trace amounts of MNZ in biological or pharmaceutical samples without complicated preconditioning. Hence, the proposed method with SDS-GR modified carbon paste electrode expected to be application in real samples.

ACKNOWLEDGEMENTS
The authors gratefully acknowledge the financial support by Guangdong Science and Technology Program（2014A040401086）and International Science and Technology Cooperation Projects of Guizhou Province（[2013]7042）and Innovation School Project of Guangdong pharmaceutical university (201530573031)

References

1. P.N. Bartlett, E. Ghoneim, G. El-Hefnawy, I. El-Hallag, *Talanta*, 66 (2005) 869.
2. J. Peng, C. Hou, X. Hu, *Sens. Actuators B: Chem.*, 169 (2012) 81.
3. Y. Wang, P. Zhang, N. Jiang, X. Gong, L. Meng, D. Wang, N. Ou, H. Zhang, *J.Chromatogr. B*, 899 (2012) 27.
4. T.G. Do Nascimento, E. de Jesus Oliveira, R.O. Macêdo, *J. Pharmaceut. Biomed.*, 37 (2005) 777.
5. J. Jeffery, Z.J. Vincent, R. M. Ayling, S. J. Lewis, *Clin. Biochem*, 50 (2017) 323.
6. X. Li, P. Guo, Y. Shan, Y. Ke, H. Li, Q. Fu, Y. Wang, T. Liu, X. Xia, *J. Chromatogr.* , 1499 (2017) 57.
7. C. Sagan, A. Salvador, D. Dubreuil, P.P. Poulet, D. Duffaut, I. Brumpt, *J.Pharmaceut.Biomed.* 38 (2005) 298.
8. M.R. El-Ghobashy, N.F. Abo-Talib, *J. Adv. Res.*, 1 (2010) 323.
9. T. Saffaj, M. Charrouf, A. Abourriche, Y. Aboud, A. Bennamara, M. Berrada, *Dyes Pigments*, 70 (2006) 259.
10. O.I. Zheltvai, I.I. Zheltvai, V.V. Spinul, V.P. Antonovich, *J. Anal. Chem.*, 68 (2013) 600.
11. 11. M. M. Issa, R.A.M. Nejem, A.M.A. Shanab, N.T. Shaat, *Spectrochim. Acta Part A.*, 114 (2013) 592.
12. M. Mehrzad-Samarin, F. Faridbod, A.S. Dezfuli, M. R. Ganjali, *Biosens. Bioelectron.*, 92 (2017) 618.
13. A. A. Salem, H.A. Mossa, B.N. Barsoum, *J. Pharmaceut. Biomed.*, 41 (2006) 654.

14. O.V. Manaenkov, A.I. Sidorov, É.M. Sul'Man, *Pharm. Chem. J.*, 37 (2003) 612.
15. N. Xiao, J. Deng, J. Cheng, S. Ju, H. Zhao, J. Xie, D. Qian, J. He, *Biosens. Bioelectron.*, 81 (2016) 54.
16. H. B. Ammar, M. B. Brahim, R. Abdelhédi, Y. Samet, *Mater. Sci. Eng. C.*, 59 (2016) 604.
17. I. Saidi, I. Soutrel, F. Fourcade, A. Amrane, N. Bellakhal, F. Geneste,*Electrochim. Acta*, 191 (2016) 821.
18. Y. Liu, J. Liu, H. Tang, J. Liu, B. X, F. Yu, Y. Li, *Sens. Actuators B: Chem.*, 206 (2015) 647.
19. D. Chen, J. Deng, J. Liang, J. Xie, C. Hu, K. Huang, *Sens. Actuators B: Chem.*, 183 (2013) 594.
20. Y. Gu, X. Yan, W. Liu, C. Li, R. Chen, L. Tang, Z. Zhang, M. Yang, *Electrochim. Acta*, 152 (2015) 108.
21. Y. B. Mollamahale, M. Ghorbani, M. Ghalkhani, M. Vossoughi, A. Dolati, *Electrochim. Acta*, 106 (2013) 288.
22. A. Salimi, M. Izadi, R. Hallaj, M. Rashidi, *Electroanal*, 19 (2007) 1668.
23. W. Liu, J. Zhang, C. Li, L. Tang, Z. Zhang, M. Yang, *Talanta*, 104 (2013) 204.
24. B. Sehatnia, R. E. Sabzi, F. Kheiri, A. Nikoo, *Eur. J. Chem.*, 6 (2015) 31.
25. L. Tang, Y. Wang, Y. Li, H. Feng, J. Lu, J. Li, *Adv. Funct. Mater.*, 19 (2009) 2782.
26. D. Zheng, J. S. Ye, W. D. Zhang, *Electroanal.*, 20 (2008) 1811.
27. L. Mao, K. Zhang, H.S. On Chan, J. Wu, *J.Mater. Chem.*, 22 (2012) 80.
28. R. Ojani, E. Tirgari, J. B. Raoof, *J Solid State Electr*, 20 (2016) 2305.
29. G. Alarcón-Angeles, S. Corona-Avendaño, M. Palomar-Pardavé, A. Rojas-Hernández, M. Romero-Romo, M.T. Ramírez-Silva, *Electrochim. Acta*, 53 (2008) 3013.
30. S. D. Lamani, R. N. Hegde, A. P. Savanur, S. T. Nandibewoor, *Electroanal.*, 23 (2011) 347.
31. A. Mao, H. Li, L. Yu, X. Hu, *J. Electroanal. Chem.*, 799 (2017) 257.
32. Y. Gu, X. Yan, C. Li, B. Zheng, Y. Li, W. Liu, Z. Zhang, M. Yang, *Biosens. Bioelectron.*, 77 (2016) 393.
33. A. Hernández-Jiménez, G. Roa-Morales, H. Reyes-Pérez, P. Balderas-Hernández, C. E. Barrera-Díaz, M. Bernabé-Pineda, *Electroanal*, 28 (2016) 704.
34. Y. Gu, W. Liu, R. Chen, L. Zhang, Z. Zhang, *Electroanal.*, 25 (2013) 1209.
35. J. Huang, X. Shen, R. Wang, Q. Zeng, L. Wang, *Rsc Adv.*, 7 (2017) 535.
36. A. M. O. Brett, S. H. P. Serrano, I. Gutz, M. A. La-Scalea, M.L. Cruz, *Electroanal.*, 14 (1997) 1132.
37. H. J. Du, J. S. Ye, J. Q. Zhang, X. D. Huang, C. Z. Yu, *Electroanal.l*, 22 (2010) 2399.
38. S. Lee, J. Oh, D. Kim, Y. Piao, *Talanta*, 160 (2016) 528.
39. S. Lee, S. Park, E. Choi, Y. Piao, *J. Electroanal. Chem.*, 766 (2016) 120.
40. W. H. Cai, T. Lai, H. J. Du, J. S. Ye, *Sens.Actuators B: Chem.*, 193 (2014) 492.
41. A. Levent, A. Altun, Y. Yardım, Z. Şentürk, *Electrochim. Acta*, 128 (2014) 54.
42. F.C. Anson, *Anal. Chem.*, 36 (1964) 313.
43. X. Zhu, K. Zhang, N. Lu, X. Yuan, *Appl. Surf. Sci.*, 361 (2016) 72.
44. Y. Li, X. Zhai, X. Liu, L. Wang, H. Liu, H. Wang, *Talanta*, 148 (2016) 362.
45. U. Bilibio, L. H. de Oliveira, V. S. Ferreira, M. A. G. Trindade, *Microchem. J.*, 116 (2014) 47.
46. C. Hu, C. Yang, S. Hu, *Electrochem. Commun.*, 9 (2007) 128.
47. P. Wiczling, P. Kawczak, A. Nasal, R. Kaliszan, *Anal. Chem.*, 78 (2006) 239.
48. K. Hu, A. J. Bard, *Langmuir*, 13 (1997) 5418.
49. D. Zheng, J. S. Ye, W. D. Zhang, *Electroanal.*, 20 (2008) 1811.
50. M. B. Gholivand, G. Malekzadeh, M. Torkashvand, *J. Electroanal. Chem.*, 704 (2013) 50.
51. Y. Selehattin, B. Esra, S. Gulsen, Y. Sultan, *J. Serb. Chem. Soc.*, 78 (2013) 295.
52. S. F. Lu, K. B. Wu, X. P. Dang, S. S. Hu, *Talanta*, 63 (2004) 653.
53. Y. Gu, W. L. Liu, R. X. Chen, L. Zhang, Z.Q. Zhang, *Electroanal. (N. Y.)*, 25 (2013) 1209.
54. W. L. Liu, J. F. Zhang, C. Li, L. Tang, Z.Q. Zhang, M. Yang, *Talanta*, 104 (2013) 204.

55. G. Yang, F. Zhao, B. Zeng, *Electrochim. Acta*, 135 (2014) 154.